Exploiting multi-lead electrocardiogram correlations using robust third-order tensor decomposition

Sibasankar Padhy ✉, *Samarendra Dandapat*

Department of Electronics and Electrical Engineering, Indian Institute of Technology Guwahati, Guwahati PIN-781 039, Assam, India
✉ *E-mail: sibasankar@iitg.ernet.in*

Published in Healthcare Technology Letters; Received on 15th April 2015; Revised on 20th July 2015; Accepted on 21st July 2015

In this Letter, a robust third-order tensor decomposition of multi-lead electrocardiogram (MECG) comprising of 12-leads is proposed to reduce the dimension of the storage data. An order-3 tensor structure is employed to represent the MECG data by rearranging the MECG information in three dimensions. The three-dimensions of the formed tensor represent the number of leads, beats and samples of some fixed ECG duration. Dimension reduction of such an arrangement exploits correlations present among the successive beats (intra-beat and inter-beat) and across the leads (inter-lead). The higher-order singular value decomposition is used to decompose the tensor data. In addition, multiscale analysis has been added for effective care of ECG information. It grossly segments the ECG characteristic waves (P-wave, QRS-complex, ST-segment and T-wave etc.) into different sub-bands. In the meantime, it separates high-frequency noise components into lower-order sub-bands which helps in removing noise from the original data. For evaluation purposes, we have used the publicly available PTB diagnostic database. The proposed method outperforms the existing algorithms where compression ratio is under 10 for MECG data. Results show that the original MECG data volume can be reduced by more than 45 times with acceptable diagnostic distortion level.

1. Introduction: E-health is one of the promising applications in today's age that provides a secure information and communication technology in support of healthcare services. These healthcare organisations may require access to physiological signals, such as electrocardiogram (ECG), electroencephalography, SpO2 etc., for future analysis. Hence, there is a need for a central repository that can store this abundant data. Recent advances in digital technologies have influenced the designing of cloud-based systems that can interact with these organisations. The overgrowing use and traffic in the cloud may have an adverse effect in accessing this data. Data volume reduction is a proposed solution to overcome this problem [1].

A WHO study shows that cardiac disorders are the primary cause of high mortality rate across the globe [2]. The symptoms of a cardiac patient are reflected in the ECG. It records the entire pumping activity of the heart, and is used to diagnose the cardiac patients. A single lead ECG provides only selective information of a heart condition in a particular view. It is also difficult to analyse all types of cardiac problems using a single lead ECG. Hence cardiologists use the standard 12-lead ECG system for critical diagnostic decision. The 12-lead ECG system henceforth is termed as multi-lead ECG (MECG). The size of MECG, containing millions of heartbeats of multiple patients, is too large to be stored in their entirety. The Letter proposed here focuses on data reduction of MECG for storage purpose.

The key idea of the proposed algorithm is to reduce the dimension by exploiting the correlations present in the MECG data without losing clinical information. There are three types of correlations, namely, intra-beat, inter-beat and inter-lead correlations [3]. Several methods that exploit inter-beat [4–6] or both intra- and inter-beat correlations [7] of a single lead ECG signal have been proposed. Recently, fractal-based single lead ECG compression has been proposed [1]. It exploits only inter-beat correlation of single lead ECG. Keeping in view the importance of the MECG data, efforts on inter-lead correlation among the leads have been carried out using multiscale principal component analysis (PCA) [8]. Cetin *et al.* [9] have exploited both intra-beat and inter-lead correlations. To the best of our knowledge, there is no Letter that makes use all three types of correlations simultaneously MECG data. The proposed method exploits all types of correlations using higher-order singular value decomposition (HOSVD). The advantages of this method are: it saves a large number of computations of floating point operations and it eases the storage scarcity problem. A preliminary version of this Letter has been reported in [10], where multilevel 3D discrete wavelet transform (DWT) (3D multiscale analysis) has been applied on the MECG tensor. It was difficult to analyse the morphological waves (P-wave, QRS-complex, ST-segment and T-wave) of the ECG signal as the 3D multiscale analysis is unable to segment these waves. Moreover, the compression performance was moderate with a compression ratio (CR) under 18. In this Letter, we have enhanced the performance by adding 1D multiscale analysis which treats ECG clinical information efficaciously. Moreover, a comparison for different cardiac disorders is presented. Results shown in this Letter are compared with the earlier works.

The rest of this Letter is organised as follows: Section 2 discusses the proposed HOSVD-based MECG data reduction scheme in wavelet domain. The results and discussion are presented in Section 3, followed by our conclusions in Section 4.

Notations: Before starting the next section, we would like to point out the notations used in this Letter. Scalars, vectors and matrices follow the standard notations. A third-order tensor of size $I \times J \times K$ is written with a calligraphic letter $\mathcal{X}$, and its elements as x_{ijk}, $i = 1, \ldots, I, j = 1, \ldots, J$ and $k = 1, \ldots, K$. The other two terminologies associated with a tensor are *fibres* and *slices*. The mode-1 fibres of the tensor are the column vectors $\boldsymbol{x}_{:jk}$, and are characterised by fixing the index in all modes except one. Mode-2 and mode-3 fibres are the row and tube vectors, and are represented as $\boldsymbol{x}_{i:k}$ and $\boldsymbol{x}_{ij:}$, respectively. Similarly, the slices of a tensor are obtained by fixing any two indexes and its structure is similar to a matrix, for example, $\boldsymbol{X}_{i::}$. The above generated slices (i fixed) are called the 'horizontal' matrices. Similarly, another two types of slices, keeping j and k fixed, are named the 'vertical' and 'frontal' matrices, respectively. Two common operations associated with a tensor are flattening and mode-n product. A tensor of order N can be unfolded or flattened in N different ways. The n-mode flattening is adopted from [11]. The n-mode fibres are the columns of the

doi: 10.1049/htl.2015.0020

n-mode flattened matrix. The flattening of a tensor $\mathcal{X}$ in its n-mode is symbolised by the matrix $\boldsymbol{X}^{(n)}$. The mode-n product of a tensor $\mathcal{X} \in \mathbb{R}^{I_1 \times I_2 \times \ldots, I_n}$ with a matrix $\boldsymbol{A} \in \mathbb{R}^{J \times I_n}$ is represented as $\mathcal{Y} = \mathcal{X} \times_n A$. In terms of the flattened tensors, the product can be expressed as $\boldsymbol{Y}^{(n)} = \boldsymbol{A}\boldsymbol{X}^{(n)}$. [In this Letter, tensor operations such as flattening, mode-n product and HOSVD etc. are performed. For these operations, we have used the MATLAB Tensor toolbox [12].]

2. Method: The block diagram of the proposed method for third-order tensor MECG is shown in Fig. 1. The encoder part comprises of preprocessing, MECG tensor data formation and multiscale HOSVD. Exploitation of three types of redundancies is achieved by representing the MECG data in third-order tensor form. Then multiscale (L-level 1D DWT) HOSVD is applied on the MECG tensor. This turns out to achieve a high data reduction volume without loss of any clinical information. Fig. 1*b* shows the decoder part of the proposed method. It follows the reverse process, that is, decoding, HOSVD restoration, IDWT, third-order tensor representation followed by period recovery and postprocessing.

2.1. Tensor MECG data formation: Tensors are used to store the multi-dimensional data. An n-dimensional tensor can be represented mathematically as $\mathcal{X} \in \mathbb{R}^{I_1 \times I_2 \times \ldots I_n}$ where n is the order of the tensor and I_d is the size of its dth dimension. The work presented in this Letter deals with third-order tensor, and the size of the tensor is discussed later.

The MECG data is a 2D matrix data where the rows represent the number of leads, and the samples of each lead can be represented as the number of columns. It can be laid out as a tensor by stacking vertical slices side-by-side, since the timing information across all the leads is the same. Each vertical slice represents a beat period of all leads. This is done by following beat detection, segmentation and period normalisation. To reduce the computational complexity, the R-peaks of two leads (V2 and V10) are detected by following the Pan-Tompkin's algorithm [13]. The PTB database, considered in this Letter, has less noise in the precordial leads; hence, V2 and V10 are considered for peak detection. The R-peak detection of a single lead may be sufficient but two leads are processed to avoid the detection of missing R-peaks during some pathological cases. An ECG beat period comprises of a P-wave, followed by a QRS-complex and finally a T-wave. The duration of the PR interval (on-set of P-wave to the beginning of the QRS-complex) is 120–200 ms. Each beat period has a length of consecutive R-peaks, and is spanned 200 ms (200 samples) left from the current R-peak to 200 ms left from the next R-peak. After detection of R-peaks, each lead is segmented and normalised to the number of beat periods. Each beat period of a lead (V2 or V10) is normalised to a same length (p) using the cubic spline interpolation technique. The size of the ECG periods of other leads is normalised to p. Then, we arranged the MECG data as third-order tensor $\mathcal{X} \in \mathbb{R}^{m \times n \times p}$, where the dimensions m, n and p are the number of leads, heart beats and consecutive samples of the period normalised heartbeat, respectively. The horizontal slices of $\mathcal{X}$ (keeping first index m fixed, whereas the two other indices, n and p, are free) represent each ECG data, and each vector of a horizontal matrix represents the consecutive beats of a lead. Similarly, a vertical slice contains the beat information of all leads.

2.2. Multiresolution analysis of MECG data: The non-stationary nature of the ECG signal incited us to use the WT, to know exactly the occurrence of different ECG morphologic features in a particular frequency sub-band. In other words, different morphologic waves of an ECG signal are grossly segmented into different sub-bands depending on their frequency content [14]. In this Letter, dyadic DWT with Daubachies 9/7 biorthogonal wavelet filters as the mother wavelet has been used. It is implemented using a multiresolution pyramidal decomposition technique. The filter bank implementation of dyadic DWT that is decomposed with L-level results in $L+1$ sub-band levels. The number of decomposition levels is chosen by using the formula $L = \lfloor \log_2 F_s - 2.96 \rfloor$ where F_s is the sampling frequency [15].

The third-order MECG tensor $\mathcal{X}_{m \times n \times p}$ is wavelet decomposed using 1D DWT. It is applied on the mode-3 fibres ($\boldsymbol{x}_{mn:}$) (by varying m and n with fixed p) to generate p-dimensional wavelet coefficients, as the 1D DWT can be applied on a vector. The resulted $L+1$ sub-band tensors comprise of one approximation ($\mathcal{A}_L$) and L number of details ($\mathcal{D}_L, \ldots, \mathcal{D}_1$) sub-band tensors. The dimensions of these tensors, $\mathcal{A}_L$ and $\mathcal{D}_j$, $j = L, \ldots 1$, are given as $m \times n \times p/2^L$ and $m \times n \times p/2^j$, respectively.

2.3. Higher-order SVD on third-order sub-band tensors: For benefit of readers, we will discuss some of the basics on SVD and

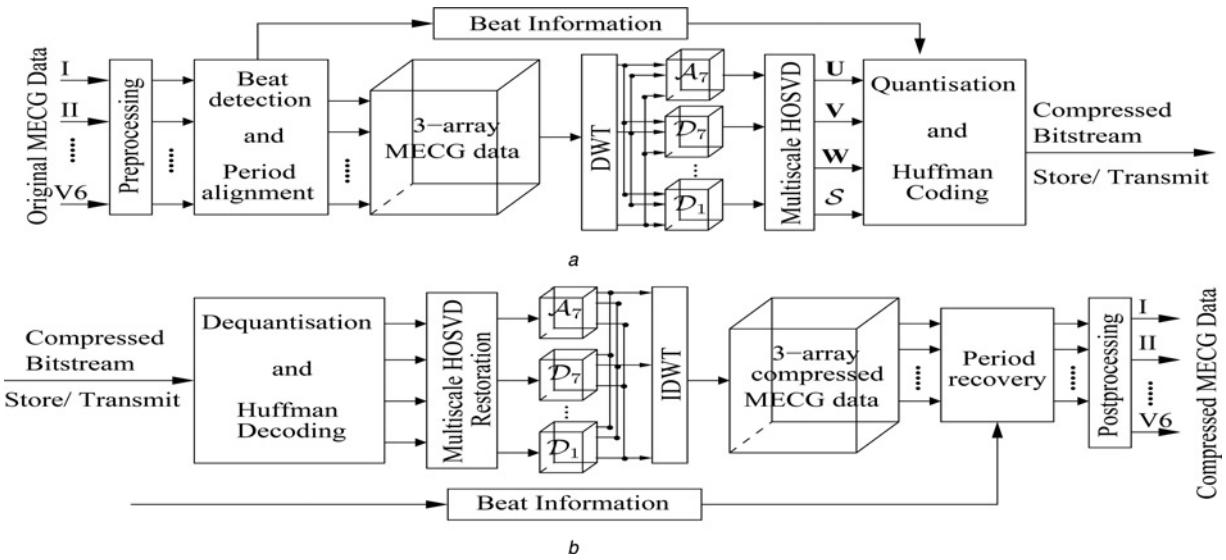

Figure 1 *Block diagram of MECG data*
a Compression
b Reconstruction

higher-order SVD (HOSVD). A detailed description on HOSVD can be found in [16].

2.3.1 Basics on HOSVD: The key idea of the SVD is to project the MECG data to a new uncorrelated space by removing the redundant information without discarding any diagnostic information. Let the MECG data matrix $\boldsymbol{X} \in \mathbb{R}^{m\times n}$ be represented as a 2-tensor where n and m represent the number of leads and number of samples of each lead, respectively. SVD decomposes it into two orthonormal matrices and a diagonal matrix as $\boldsymbol{X} = \boldsymbol{U}\boldsymbol{\Sigma}\boldsymbol{V}^{\mathbf{T}}$ where $\boldsymbol{U} \in \mathbb{R}^{m\times m}$, $\boldsymbol{V} \in \mathbb{R}^{n\times n}$ and $\boldsymbol{\Sigma}_{m\times n} = [\text{diag}\{\sigma_1, \ \ldots, \ \sigma_n\}{:}0]$, $\sigma_1 \geq \ \cdots \ \geq \sigma_n \geq 0$ and $\sigma_1, \ \ldots, \ \sigma_n$ are the singular values. The reduced-SVD on $\boldsymbol{X}$ is $\boldsymbol{X} = \hat{\boldsymbol{U}}\hat{\boldsymbol{\Sigma}}\boldsymbol{V}^{\mathbf{T}}$ where $\hat{\boldsymbol{U}} \in \mathbb{R}^{m\times n}$, $\hat{\boldsymbol{\Sigma}} \in \mathbb{R}^{n\times n}$ and $\boldsymbol{V} \in \mathbb{R}^{n\times n}$. $\hat{\boldsymbol{U}}$ and $\boldsymbol{V}$ represent the column and row spaces of the MECG data, respectively [17]. In other words, the generated $\hat{\boldsymbol{U}}$ and $\boldsymbol{V}$ represent the intra-beat and inter-lead variations. Dimension reduction of $\boldsymbol{X}$ is performed by selecting $k(k<n)$ significant singular values, and the approximation of $\boldsymbol{X}$ is represented as $\tilde{\boldsymbol{X}} \approx \sum_{i=1}^{k} \boldsymbol{\sigma}_i \boldsymbol{u}_i \boldsymbol{v}_i^{\mathbf{T}}$.

The SVD of a matrix can be generalised to a tensor of any dimension using the HOSVD [16, 18, 19]. Visualisation and approximation of HOSVD is presented in Fig. 2. We have limited our discussion to a third-order tensor $\mathcal{X}_{m\times n\times p}$, which can be decomposed using HOSVD as

$$\mathcal{X} \ = \mathcal{S}\times_1 \boldsymbol{U} \times_2 \boldsymbol{V} \times_3 \boldsymbol{W} \tag{1}$$

where $\boldsymbol{U} \in \mathbb{R}^{m\times m}$, $\boldsymbol{V} \in \mathbb{R}^{n\times n}$ and $\boldsymbol{W} \in \mathbb{R}^{p\times p}$ are orthonormal matrices. These matrices ($\boldsymbol{U}$, $\boldsymbol{V}$ and $\boldsymbol{W}$) are obtained via SVD as these represent the left singular matrices of $\boldsymbol{X}^{(n)}$. However, we can save a large number of floating point operations without calculating the right singular matrices. After obtaining the orthonormal matrices, the core tensor $\mathcal{S}$ is computed as $\mathcal{S} = \mathcal{X}\times_1 \boldsymbol{U}^{\mathrm{T}} \times_2 \boldsymbol{V}^{\mathrm{T}} \times_3 \boldsymbol{W}^{\mathrm{T}}$. It corresponds to the singular value matrix of conventional 2D SVD, although it does not have a simple diagonal structure [17].

The core tensor $\mathcal{S}$ has the dimension as that of $\mathcal{X}$. Typical rank of a tensor ($\mathcal{X}$) of size $m \times n \times p$ with $mn \leq p$ is mn [11]. Hence, first mn frontal slices of the core tensor have significant non-zero values and rest $p' = p - mn$ frontal slices have very small numbers in the order of 10^{-12} or less which can be set to zero. The effective dimension of core tensor $\mathcal{S}$ is $m \times n \times p'$ and satisfies the following properties:

- *All-orthogonal* [16], that is, any two slices in a fixed mode are orthogonal.

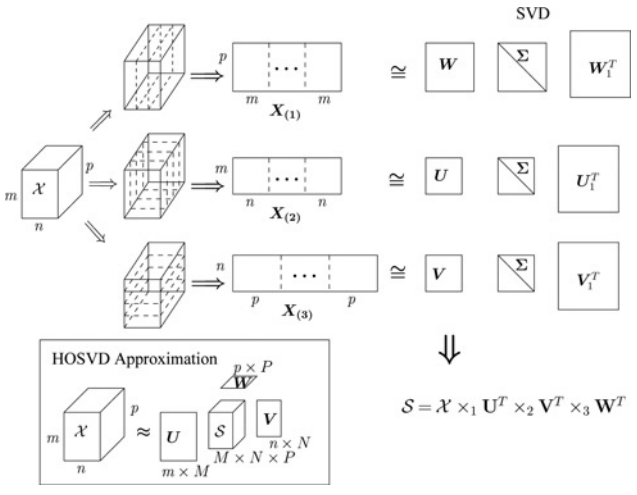

Figure 2 *HOSVD visualisation and approximation for a third-order tensor*

- *Ordered* [16], that is, the norms of the slices along any mode are ordered in a decreasing manner. For example

$$\text{first mode: } ||\mathcal{S}(1, \ :, \ :)|| \geq ||\mathcal{S}(2, \ :, \ :)|| \geq \cdots \geq 0 \tag{2}$$

The above ordered property informs about the energy of the core tensor. It is concentrated in the s_{111} element. This is the reason why HOSVD is used for data compression.

As discussed earlier for SVD case, the mode matrices $\boldsymbol{U}$, $\boldsymbol{V}$ and $\boldsymbol{W}$ contain the orthonormal vectors. These vectors span the column space of three different types of slices that resulted from the flattening of $\mathcal{X}$ along different modes. For example, the left orthogonal matrix $\boldsymbol{U}$ is calculated by applying SVD on the $m \times np$ matrix which is obtained by mode-1 flattening of $\mathcal{X}$. These mode matrices are regularised by the core tensor $\mathcal{S}$.

The basic motive of this Letter is the low rank approximation of the tensor $\mathcal{X}$ that makes use of the redundancy present between successive beats of each lead, that is, inter-beat correlation in addition to the other two. To have the core tensor $\mathcal{S}$ as a compression of $\mathcal{X}$, reduced dimensions can be chosen as $M \ll m$, $N \ll n$ and $P \ll p'$. Hence, $\mathcal{X}$ can be approximated as

$$\mathcal{X} \ \approx \hat{\mathcal{S}}\times_1 \hat{\boldsymbol{U}} \times_2 \hat{\boldsymbol{V}} \times_3 \hat{\boldsymbol{W}} \tag{3}$$

where $\hat{\mathcal{S}} \in \mathbb{R}^{M\times N\times P}$, $\hat{\boldsymbol{U}} \in \mathbb{R}^{m\times M}$, $\hat{\boldsymbol{V}} \in \mathbb{R}^{n\times N}$ and $\hat{\boldsymbol{W}} \in^{p'\times P}$, respectively.

2.3.2 HOSVD application on sub-band tensors: After having a brief idea of HOSVD, let us discuss the application of HOSVD on $L+1$ multiscale tensors (Section 2.2) for dimensionality reduction. These tensors can be decomposed as

$$\mathcal{A}_L = \mathcal{S}_{A_L} \times_1 \boldsymbol{U}_{\boldsymbol{A_L}} \times_2 \boldsymbol{V}_{\boldsymbol{A_L}} \times_3 \boldsymbol{W}_{\boldsymbol{A_L}} \tag{4}$$

$$\mathcal{D}_j = \mathcal{S}_{D_j} \times_1 \boldsymbol{U}_{\boldsymbol{D_j}} \times_2 \boldsymbol{V}_{\boldsymbol{D_j}} \times_3 \boldsymbol{W}_{\boldsymbol{D_j}} \tag{5}$$

The discussion and properties presented in the previous Section 2.3.1 are applicable to each multiscale tensor. The column vectors of $\boldsymbol{U}_{\boldsymbol{A_L}}$ and $\boldsymbol{U}_{\boldsymbol{D_j}}$ span the lead space in respective sub-bands. The column vectors of $\boldsymbol{V}_{\boldsymbol{A_L}}$ and $\boldsymbol{V}_{\boldsymbol{D_j}}$ span the beat space and the column vectors of $\boldsymbol{W}_{\boldsymbol{A_L}}$ and $\boldsymbol{W}_{\boldsymbol{D_j}}$ span each beat sample space in respective sub-bands [17]. Owing to the multiresolution property of the DWT, the morphological features of the ECG signal are grossly segmented into different wavelet sub-bands depending on their frequency content. Hence, the significant information of each beat of different leads are encoded in different orthogonal sub-band matrices.

The dimension of core tensors corresponding to $\mathcal{A}_7$, $\mathcal{D}_7$ and $\mathcal{D}_6$ are kept as these tensors contribute ~84% ($\mathcal{A}_7$: 36.47%, $\mathcal{D}_7$: 24.82% and $\mathcal{D}_6$: 22.61%) altogether of the total relative energy. Energy corresponds to the squared Frobenius-norm [Evaluation of Frobenius-norm and squared n-mode singular values can be found in [16].] of a tensor. As the D_1 sub-band has frequency information from 250 to 500 Hz, this sub-band core tensor has been discarded. Other sub-band tensors ($\mathcal{D}_5 \cdots \mathcal{D}_2$) have been processed for further dimensionality reduction. This has been performed by measuring the quality of approximation of these tensors. The decreasing nature of the n-mode singular values of each sub-band tensor can be used as a measure for the approximation [16, Property 10]. Frobenius-norm based dimensionality reduction has been used in [20]. Similarly, we have used the squared n-mode singular values of each sub-band as the thresholding parameter. Owing to the ordering property of the norms of slices, each multiscale tensor can be approximated by discarding non-significant singular value of core tensors $\mathcal{S}_{D_5} \cdots \mathcal{S}_{D_2}$ and corresponding vectors of orthogonal matrices. Hence, the values of M, N and P for each multiscale tensor can

doi: 10.1049/htl.2015.0020

be chosen using the following thresholding technique

$$\eta_j^{(k)} = \frac{\sum_{i=1}^{I_k} (\sigma_i^{(k)})^2}{||\mathcal{S}_{D_j}||_F^2} > 0.95 \quad (6)$$

where $j = 2, 3, 4$ and 5 for respective sub-band tensors, $I_k = M$ or N or P depending on the mode and $||\mathcal{S}_{D_j}||_F^2 = \sum_i^m (\sigma_i^{(1)})^2 = \sum_i^n (\sigma_i^{(2)})^2 = \sum_i^{p'} (\sigma_i^{(3)})^2$. p' is the third-order dimension of each multiscale tensor and it varies as discussed in Section 2.2.

3. Results and discussion: In this Section, the data reduction performance of the proposed method in terms of CR and three distortion measures, with a comparative study on few existing methods, is presented. For evaluation purposes, MECG data is considered from the PTB diagnostic ECG database [21]. It contains 549 records of 290 subjects of different diagnostic classes. There is no clinical summary for 22 subjects. The other 268 subjects are classed as follows: myocardial infarction (148), cardiomyopathy (18), bundle branch block (15), dysrhythmia (14), myocardial hypertrophy (7), valvular heart disease (6), myocarditis (4), healthy control (52) and others (4). Each record includes 15 continuous recorded signals: the conventional 12-leads and 3 Frank leads. Each signal is digitised at 1000 samples per second, with 16-bit resolution. The data of standard 12-leads is used. This Letter is a frame-wise processing of ECG beats where each frame contains B number of beats, and frames of limited records have been considered as shown in Table 1. CR increases with the number of beats but we have fixed $B = 10$. The number of frames considered from different diagnostic classes for our analysis is shown in Table 1.

The multiscale HOSVD is applied on each sub-band tensor as described in Section 2. To avoid any loss of low-frequency characteristics in ECG, information in higher sub-band tensors is kept intact, that is, the dimension of core tensors ($\mathcal{A}_7$, $\mathcal{D}_7$ and $\mathcal{D}_6$) are fully retained. It has been observed that the relative energy of core tensor $\mathcal{D}_1$ is 0.06%. This is because it does not carry any ECG information and contains noise or motion artefacts. Overall, clinical information of the processed signal has not been affected much by discarding this sub-band tensor. This also helps in faster processing as a minimum of 50% of wavelet transformed coefficients are eliminated which are present in this sub-band tensor. The dimension of other core tensors are reduced using the thresholding technique given in (6). It is observed that the mode-1 and the mode-2 dimensions of core tensors ($\mathcal{S}_{D_5}$, ... $\mathcal{S}_{D_2}$) reduced to 7.3 and 6.7 (on an average) from 12 and 10, respectively. Moreover, there is a large dimensional reduction in mode-3 dimensions of $\mathcal{S}_{D_3}$ and $\mathcal{S}_{D_2}$ core tensors. It has been observed during simulation for a dataset that, due to the rank property of the tensor as discussed earlier, the mode-3 dimension of $\mathcal{S}_{D_2}$ having original size ($12 \times 10 \times 223$) is reduced from 223 to 120 and further to 5 due to the thresholding technique. Similarly, it reduced to 8 from 116 for $\mathcal{S}_{D_3}$ after thresholding.

Fig. 3 shows the original (upper row) and compressed (lower row) ECG signals of leads I, aVR and V6. Owing to page constraints, we have not shown all 12-leads. It is clear that ECG characteristic waves are well preserved. Moreover, in I and aVR we can mark that noise has been reduced significantly in the compressed signals. This is due to application of multiscale DWT where the high-frequency sub-band tensors have been reduced.

3.1. Compressed MECG performance: The compression performance is evaluated using average CR and distortion measures such as percentage root mean square difference (PRD) [15], weighted diagnostic distortion (WDD) [22] and wavelet energy-based diagnostic distortion (WEDD) [14]. CR is the ratio of number of bits required to represent the signal before and after data size reduction. Bits for reduced data size include the number of bits required to represent non-zero coefficients, dictionary information, corresponding significance map and header information [23]. Of the three objective distortion measures used to evaluate the performance in this Letter, WDD and WEDD are diagnostic distortion measures, whereas PRD is a non-diagnostic measure [14, 15, 22].

The significant singular vector coefficients (vectors containing non-zero elements of $\boldsymbol{U}$, $\boldsymbol{V}$, $\boldsymbol{W}$ and $\mathcal{S}$) are uniformly quantised with 8-bit quantisation level, and corresponding CR values are calculated. The vector containing non-zero indices of core tensor $\mathcal{S}$ are quantised with 14 bits, whereas the vectors containing non-zero indices of $\boldsymbol{U}$, $\boldsymbol{V}$ and $\boldsymbol{W}$ are quantised with 8 bits.

To verify how well the clinical morphological features are preserved after compression, the distortion measures, namely, PRD, WDD and WEDD are evaluated. In [22], Zigel *et al.* considered 18 features (six each from the duration, the shape and the amplitude parameters) and a penalty matrices with a weighted diagonal matrix for WDD evaluation. The same procedure has been adopted in this Letter. First, WDD is evaluated for each beat. Then these values are averaged for different leads. The average values of the distortion measures with CR for some datasets are enlisted in Table 1. Data shown here is of average values from different diagnostic classes.

Table 1 Average CR and distortion measures of different diagnostic classes

Diagnostic classes	Number of frames	Metric	I	II	III	aVR	aVL	aVF	V1	V2	V3	V4	V5	V6	CR
Myocardial infarction	20	PRD	11.85	5.98	3.92	28.75	7.07	24.87	5.18	3.25	3.49	2.39	4.23	3.52	46.3
		WDD	3.52	1.94	1.89	4.61	2.18	3.84	1.77	1.63	1.72	0.98	1.85	1.64	
		WEDD	4.39	2.56	2.29	6.57	2.64	5.48	3.51	2.37	2.91	1.88	2.27	2.92	
Cardiomyopathy	17	PRD	9.71	4.53	2.49	27.42	3.72	23.19	3.82	2.54	2.96	2.99	3.77	3.28	42.6
		WDD	3.01	1.88	1.47	4.79	1.79	4.47	1.82	1.31	1.56	1.32	1.94	1.57	
		WEDD	3.81	2.51	2.17	6.79	2.44	5.26	3.07	2.16	2.43	1.99	2.11	2.81	
Bundle branch block	17	PRD	10.55	4.13	2.19	27.56	4.72	25.47	4.19	2.64	3.28	2.97	3.61	3.34	45.7
		WDD	3.15	1.83	1.33	5.07	1.93	4.76	1.86	1.06	1.34	1.25	1.99	2.02	
		WEDD	4.07	2.60	2.15	6.03	2.06	5.20	3.14	2.14	2.29	2.10	2.31	2.02	
Dysrhythmia	16	PRD	12.81	5.84	3.29	29.53	4.28	26.71	4.17	3.57	3.91	2.94	3.76	3.94	26.3
		WDD	3.42	1.60	1.37	5.23	1.94	5.16	2.21	1.88	2.09	1.19	1.95	2.35	
		WEDD	4.79	4.36	3.85	8.72	4.84	5.41	3.68	3.49	3.82	2.74	2.90	3.05	
Healthy control	17	PRD	9.12	3.97	2.89	27.18	4.11	26.69	3.26	3.13	2.41	2.38	4.19	3.17	49.1
		WDD	3.02	2.81	1.27	5.08	2.04	4.91	1.97	1.80	0.97	1.02	1.82	1.49	
		WEDD	3.24	2.16	2.08	5.61	2.33	4.66	2.74	1.91	2.04	1.42	1.83	2.62	

The values shown in the table are for 8 bit quantisation level.

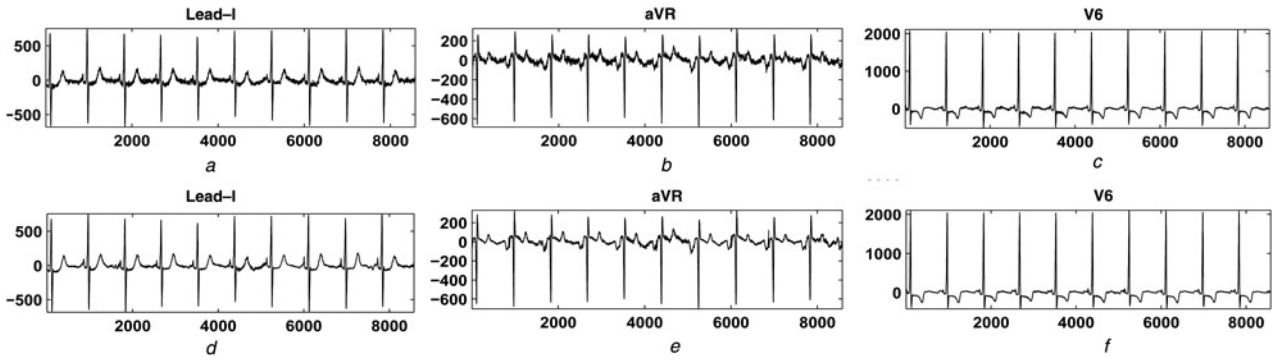

Figure 3 *Original (upper row) and compressed (lower row) ECG signals of leads I, aVR and V6*
a–c Original
d–f Compressed ECG signals of Lead-I, aVR and V6

It is observed that chest leads (V2–V6) have less PRD and WEDD, and fall under an 'excellent' (0–4.33) or 'very good' (4.33–7.8) category [15]. In any diagnostic class, we observed that the PRD values of bipolar and augmented leads are higher than the chest leads which may be due to the presence of motion artefacts and noise. The high PRDs (>24) in leads aVR and aVF do not signify poor reconstruction quality, rather it is due to removal of noise in these leads [see Fig. 3]. Discussing the WDD, values that are smaller than 2.3 suggest the preservation of clinical information. These fall under the 'very good' category ($0 - 2.3$ [22]). Some leads (I, aVR and aVF) have high WDD values that fall under the 'good' category. These high values are due to the inaccurate detection of some characteristic features in those noisy leads. The low WEDD values in these leads indicate the good reconstruction quality. These values fall in the 'very good' (4.51–6.91) category. With this acceptable distortion ranges, the CR in different diagnostic classes is more than 45:1. However, for dysrhythmia class, the CR reduced to ~25:1. This may be due to an irregular nature of the heart beat where our QRS detection algorithm fails to detect the exact R-peaks. This causes the number of beats to be very high, considering the same number of ECG samples, that is, value of n becomes more than 70 instead of 8–20. This problem can be solved by an efficient QRS detection algorithm for dysrhythmia or a similar type of diagnostic classes.

3.2. Comparison with existing data reduction methods: Comparison performance of the proposed method and the existing compression techniques is carried out and is shown in Table 2. CR depends on factors such as correlation, number of leads, sampling frequency and quantisation bits/sample. There are limited works available in the literature for MECG data. The compression performance has been carried out with different databases. Hence, direct comparison of the proposed method with others may not be appropriate. For fairness in comparison, same number of frames are processed by simulating the existing algorithms. Values shown in this table are average of 87 subjects (from different diagnostic classes). The average PRD and WEDD measures shown in this table are of a single lead (V4). During simulation, it is observed that CR value decreases when number of ECG signals are increased. The KLT- and DCT-based methods have a CR of 7.25 with a PRD and WEDD of 3.18 and 3.10%, respectively. The truncated SVD algorithm has a CR of 15.7 with a PRD and WEDD of 2.83 and 2.73%, respectively. However, one can mark significant deviations in characteristic waves such as P-wave, ST-segment and T-wave of original and compressed signals [6]. This may be due to poor handling of ECG characteristic waves. Wavelet-based LP model [5] has a good data reduction capability (CR = 22.7) but has high distortion errors (PRD = 10.25% and WEDD = 6.81%). The multiscale-based PCA algorithm has less CR (12.61%) but has a good reconstruction quality with PRD and WEDD of 2.66 and 2.18%, respectively. From this table, it is clear that our proposed method outperforms the existing techniques [8, 9]. It achieved a minimum CR value of 45 (except dysrhythmia class) with PRD and WEDD of 2.71 and 2.09%, respectively.

Table 2 Comparison with existing ECG compression methods

Method	Type of correlation	CR	PRD, %	WEDD, %
Cetin *et al.* [9] (KLT and DCT)	intra-beat	7.25:1	3.18	3.10
Wei *et al.* [6] (truncated SVD)	inter-beat	15.7:1	2.83	2.73
Ramakrishnan and Saha [5] (wavelet-based LP)	inter-beat	22.70:1	10.25	6.81
Sharma *et al.* [8] (DWT-based MSPCA)	inter-lead	12.61:1	2.66	2.18
DWT-based HOSVD	all	15.09:1	3.02	2.92
proposed method multiscale HOSVD	all	>45:1	2.71	2.01

All algorithms computed in same environment (MATLAB, i5 central processing unit, 3.2 GHz processor) with equal MECG frames ($B = 10$).

4. Conclusion: In this Letter, a robust third-order tensor representation of MECG data has been proposed for cloud-based ECG monitoring systems. This type of arrangement helps exploit intra-beat, inter-lead redundancies with inter-beat which is a huge source of redundancy. The multiscale HOSVD is applied on the tensor data. HOSVD reduces the data dimension and multiscale property treats ECG information effectively. The compression performance and distortion measures of the proposed method are evaluated by measuring average CR, PRD and WEDD. The results are compared with existing compression techniques. The storage efficiency has been enhanced 45 times more with acceptable distortion label using the proposed method.

5. Declaration of interests: Conflict of interest: none declared.

6 References

[1] Ibaida A., Al-Shammary D., Khalil I.: 'Cloud enabled fractal based ECG compression in wireless body sensor networks', *Fut. Gener. Comput. Syst.*, 2014, **35**, pp. 91–101
[2] Available at http://www.who.int/topics/cardiovascular_diseases/en/index.html

doi: 10.1049/htl.2015.0020

[3] Jalaleddine S., Hutchens C., Stratran R., Coberly W.: 'ECG data compression techniques – a unified approach', *IEEE Trans. Biomed. Eng.*, 1990, **37**, (4), pp. 329–343
[4] Bradie B.: 'Wavelet packet-based compression of single lead ECG', *IEEE Trans. Biomed. Eng.*, 1996, **43**, (5), pp. 493–501
[5] Ramakrishnan A.G., Saha S.: 'ECG coding by wavelet-based linear prediction', *IEEE Trans. Biomed. Eng.*, 1997, **44**, (12), pp. 1253–1261
[6] Wei J., Chang C., Chou N., Jan G.: 'ECG data compression using truncated singular value decomposition', *IEEE Trans. Inf. Technol. Biomed.*, 2001, **5**, (4), pp. 290–299
[7] Lee H., Buckley K.M.: 'ECG data compression using cut and align beats approach and 2-D transforms', *IEEE Trans. Biomed. Eng.*, 1999, **46**, (5), pp. 556–564
[8] Sharma L.N., Dandapat S., Mahanta A.: 'Multichannel ECG data compression based on multiscale principal component analysis', *IEEE Trans. Inf. Technol. Biomed.*, 2012, **16**, (4), pp. 730–736
[9] Cetin A.E., Koymen H., Aydin M.C.: 'Multichannel ECG data compression by multirate signal processing and transform domain coding techniques', *IEEE Trans. Biomed. Eng.*, 1993, **40**, (5), pp. 495–499
[10] Padhy S., Dandapat S.: 'A new multilead ECG data compression method using higher-order singular value decomposition'. 20th National Conf. on Communications (NCC), February 2014, pp. 1–4
[11] Kolda T.G., Bader B.W.: 'Tensor decompositions and applications', *SIAM Rev.*, 2009, **51**, (3), pp. 455–500
[12] Bader B.W., Kolda T.G., *ET AL.*: 'MATLAB tensor toolbox version 2.6', February 2015. Available at http://www.sandia.gov/tgkolda/TensorToolbox/
[13] Pan J., Tompkins W.J.: 'A real-time QRS detection algorithm', *IEEE Trans. Biomed. Eng.*, 1985, **32**, (3), pp. 230–236
[14] Manikandan M.S., Dandapat S.: 'Wavelet energy based diagnostic distortion measure for ECG', *Biomed. Signal Process. Control, Elsevier*, 2007, **2**, pp. 80–96
[15] Al-Fahoum A.S.: 'Quality assessment of ECG compression techniques using a wavelet-based diagnostic measure', *IEEE Trans. Inf. Technol. Biomed.*, 2006, **10**, (1), pp. 182–191
[16] De Lathauwer L., De Moor B., Vandewalle J.: 'A multilinear singular value decomposition', *SIAM J. Matrix Anal. Appl.*, 2000, **21**, (4), pp. 1253–1278. Available at http://www.dx.doi.org/10.1137/S0895479896305696
[17] Vasilescu M., Terzopoulos D.: 'Multilinear (tensor) image synthesis, analysis, and recognition [exploratory dsp]', *IEEE Signal Process. Mag.*, 2007, **24**, (6), pp. 118–123
[18] Bergqvist G., Larsson E.G.: 'The higher-order singular value decomposition: theory and an application', *IEEE Signal Process. Mag.*, 2010, **27**, (3), pp. 151–154
[19] Savas B., Eldén L.: 'Handwritten digit classification using higher order singular value decomposition', *Pattern Recognit.*, 2007, **40**, (3), pp. 993–1003
[20] Kuang L., Hao F., Yang L., Lin M., Luo C., Min G.: 'A tensor-based approach for big data representation and dimensionality reduction', *IEEE Trans. Emerg. Top. Comput.*, 2014, **2**, (3), pp. 280–291
[21] Goldberger A.L., Amaral L.A.N., Glass L., *ET AL.*: 'Physiobank, physiotoolkit, and physionet: components of a new research resource for complex physiologic signals', *Circulation*, 2000, **101**, (23), pp. e215–e220, Circulation Electronic Pages. Available at http://www.circ.ahajournals.org/cgi/content/full/101/23/e215
[22] Zigel Y., Cohen A., Katz A.: 'The weighted diagnostic distortion (WDD) measure for ECG signal compression', *IEEE Trans. Biomed. Eng.*, 2000, **47**, (11), pp. 1422–1430
[23] Manikandan M.S., Dandapat S.: 'Wavelet threshold based ECG compression using USZZQ and Huffman coding of DSM', *Biomed. Signal Process. Control, Elsevier*, 2006, **1**, pp. 261–270